International Conference on Applied Energy 2021
Nov. 29 - Dec. 2, 2021, Thailand/Virtual
Paper ID: 541

Performance Analysis of Shell-and-tube Supercritical CO_2 Gas Heater in a CO_2 Power Generation System

Xinyu Zhang, Yunting Ge*
School of the Built Environment and Architecture
London South Bank University, 103 Borough Road, London , SE1 0AA, UK
E-mail: yunting.ge@lsbu.ac.uk

ABSTRACT

Detailed Computational Fluid Dynamics (CFD) simulation model of a particular designed shell-and-tube supercritical CO_2 gas heater in a biomass-CO_2 power generation system has been developed based on actual heat exchanger structural data. The model has been validated with both manufacturer data and empirical correlations. It is thus applied to investigate and predict the performance of the heat exchanger and its associated system at various operating conditions. Based on the CFD simulation results, the performance improvement strategies for the heat exchanger designs and system controls are found and recommended.

Keywords: shell-and-tube CO_2 gas heater, biomass-CO_2 power generation system, Computational Fluid Dynamics (CFD) modelling, performance analysis.

NONMENCLATURE

Abbreviations	
cp	heat specific ($J.kg^{-1}.K^{-1}$)
d	diameter (m)
h	heat transfer coefficient ($W.m^{-2}.K^{-1}$)
k	thermal conductivity($W.m^{-1}.K^{-1}$)
L	heat transfer length of tubes (m)
$\dot{m}$	mass flow rate($kg.s^{-1}$)
Q	heat transfer rate (kW)
T	temperature (K),
ΔT	temperature difference (K)
U	overall heat transfer coefficient ($W.m^{-2}.K^{-1}$)
Symbols/subscripts	
av	average
i	inner
o	outer
t	tube side
s	shell side

1. INTRODUCTION

Currently, fossil fuels are still the dominate primary energy resources for power generation worldwide which have brought serious concerns for environment protection. The decarbonized power generation with renewables such as biomass is becoming more and more important. Correspondingly, a CO_2 transcritical Brayton cycle can be one of the applicable options for power generation with the heat source from high temperature biomass combustion. As a main component in the power generation system, a supercritical CO_2 gas heater plays an important role in the system performance. Considering the high temperature and high pressure involved in the working fluids, a shell-and-tube type heat exchanger can be a feasible gas heater used in the system.

Shell-and-tube heat exchangers have been widely applied in industries and energy systems such as refrigerant and heat pump due to their simple design, compactness, and relative high performance. However, their operation efficiency needs be further improved with optimal designs in terms of baffle spacings, baffle cut ratios and tube arrangements etc. An experimental investigation was conducted by Kim and Aicher [1] to examine the heat transfer behaviors of a shell-and-tube heat exchanger by varying its geometries parameters. It was found that the effect of tube pitch can be neglected. In addition, for the heat exchangers with short tube length, the shell-side fluid heat transfer coefficient in tube nozzle region was much higher than that of tube parallel region. Furthermore, Halle et al. [2] measured shell-side fluid pressure drops of shell-and-tube heat exchangers with different baffle configurations. Results showed that closer baffle spacing led to higher fluid flow velocity and enhanced heat

Selection and peer-review under responsibility of the scientific committee of the 13th Int. Conf. on Applied Energy (ICAE2021).

transfer but higher pressure drops. Similar conclusions were also obtained by Sparrow and Reifschneider [3].

On the other hand, Bell-Delaware Method [4] and Kern Method [5] are two most common methods to calculate theoretically the fluid heat transfer coefficient and pressure drop on the fluid shell side. It should be noted that Kern's method can be applied to predict preliminarily the performance of shell-side fluid. However, the Bell-Delaware method is more accurate to predict the heat transfer performance of fluid shell side since the effects of leakage and bypass streams on shell side fluid are considered. Based on the correlations and equations from Bell-Delaware method, Gaddis and Gnielinski [6] evaluated and updated the shell side pressure drop calculations.

From the experimental and theoretical investigations, the heat exchanger heat transfer and hydraulic behaviors are strongly affected by the heat exchanger designs such as the baffle spacings. Nevertheless, to the authors' knowledges, there are fewer experimental and detailed theoretical investigations on the proposed biomass flue gas heated supercritical CO_2 shell-and-tube gas heater. Subsequently, in this study, a detailed CFD model for the CO_2 supercritical gas heater has been developed, validated, and simulated at different operating conditions. The simulation results can be applied for the optimal designs of the heat exchanger and system controls.

2. SYSTEM DESCRIPTION

As shown in Fig. 1, the whole system consists of several important components including a biomass heater, a CO_2 shell-and-tube gas heater, a needle valve , two gas coolers, a recuperator, a compressor, and a water cooler.

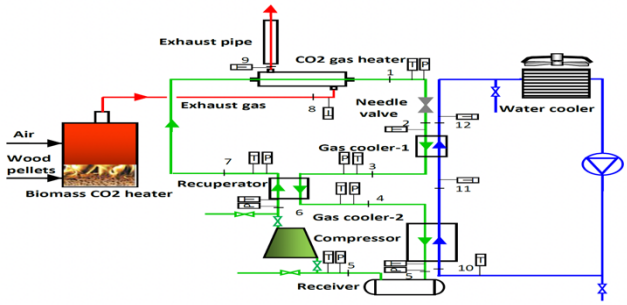

Fig. 1. Schematic diagram of Biomass-CO_2 power generation system

It is noted that a combination of the needle valve and gas cooler-1 acts as a CO_2 turbine simulator. The system operates under CO_2 transcrtical Brayton cycle. The high temperature flue gas from the biomass combustion heater passes through the CO_2 gas heater to heat the supercritical CO_2 fluid to a high temperature. The CO_2 is then expanded in the turbine simulator to generate power before releasing heat to the recuperator. After that, the CO_2 at a subcritical pressure further releases heat through the gas cooler-2 before entering the transcritical compressor to be pressured up. It then absorbs heat through the recuperator before being heated again by the gas heater. The cycle thus repeats. Some important system design parameters include flue gas temperature at 800 °C and mass flow rate at 0.12 kg/s, CO_2 turbine inlet temperature at 500°C, pressure at 120 bar and mass flow rate at 0.1272 kg/s, and CO_2 turbine outlet pressure at 50.875 bar. Based on this designed operating condition, the CO_2 gas heater is singled out and analyzed purposely.

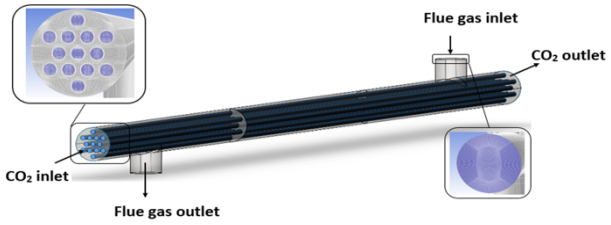

Fig. 2. The physical and mesh model of the simulated shell-and-tube heat exchanger

3. DATA REDUCTION

The total heat transfer rates of shell and tube sides can be calculated in Eq.(1) and Eq.(2) respectively.

$$Q_s = \dot{m}_s cp_s(T_{s,i} - T_{s,o}) \quad \text{Eq.(1)}$$

$$Q_t = \dot{m}_t cp_t(T_{t,o} - T_{t,i}) \quad \text{Eq.(2)}$$

The overall heat transfer coefficient is calculated in Eq. (3), in which the average heat transfer rate is calculated in Eq. (4).

$$U = \frac{Q_{av}}{\pi d_o L \Delta T} \quad \text{Eq.(3)}$$

$$Q_{av} = \frac{Q_s + Q_t}{2} \quad \text{Eq.(4)}$$

The shell side fluid flow heat transfer coefficient can be determined by Eq. (5).

$$h_s = \frac{1}{\frac{1}{U} - \frac{1}{h_t}\frac{d_o}{d_i} - \frac{d_o}{2k} ln\frac{d_o}{d_i}} \quad \text{Eq.(5)}$$

,where h_t is the tube side heat transfer coefficient calculated by CFD.

4. CFD MODEL DEVELOPMENT

4.1 Physical model

A three-dimensional geometrical model of the counterflow type CO_2 gas heater is developed by SOLIDWORKS 2019, as shown in Fig.2. Biomass flue gas flows on the shell side while CO_2 flows through the tubes. To simplify the modelling process, airflow is selected to represent the biomass flue gas. As depicted, the CO_2 gas heater consists of 2 baffles and 13 inner tubes with tube length of 3.472 m each, while the diameters of shell pipe and tube are 101.6 mm and 13.7 mm respectively.

4.2 Meshing of geometry

The CO_2 gas heater is meshed in Ansys ICEM CFD 19.2 with hexahedral type elements as indicated in Fig.2. After mesh sensitivity test, the number of mesh elements is finalized as 3,204,918. The meshed model is then loaded into Ansys Fluent 19.2 to simulate the shell side and tube side heat transfer characteristics.

4.3 Boundary conditions and solution methodologies

For turbulent flow model, realizable k-ε model, is selected for the model simulation. The CO_2 and air properties are all calculated and correlated with software REFPROP 8.0 and then loaded into Fluent via User Define Function (UDF).

Flue gas inlet temperature and velocity are applied as shell side inlet boundary condition. Similarly, CO_2 inlet temperature and velocity are applied as tube side inlet boundary condition. For shell side outlet, pressure outlet is selected with pressure set to atmospheric pressure. For the outlet pressure of tube side, it sets to vary from 8 MPa to 28 MPa. The model is simulated under different operating conditions, including flue gas mass flow rate in the range of 0.08 - 0.18 kg/s, CO_2 mass flow rate from 0.08 to 0.14 kg/s while the flue gas temperature varies from 873.15 K to 1273.15 K.

The simple scheme is selected for pressure-velocity coupling. The convergence criterion is taken as energy residual less than 10^{-7} and all other residuals are less than 10^{-3}.

5. MODEL VALIDATION

For the calculations of fluid shell-side heat transfer coefficient and pressure drop, at the same operating conditions, the CFD simulation results are compared with those calculated by Bell-Delaware Method [4] , as shown in Fig. 3(a). As depicted, the maximum deviations between these two calculations for flue gas heat transfer coefficient and pressure drop are 5.6% and 11.4% respectively. For the tube side heat transfer coefficient and pressure drop, the comparisons are made between the CFD simulation and the calculation by the empirical correlations of Gnielinski's [7], as shown in Fig. 3(b). The maximum deviations for the CO_2 heat transfer coefficient and pressure calculations are 7.1% and 9.1% respectively. In addition, at the designed operating condition, the calculated heat exchanger heating capacity is 34.24 kW by the CFD model, compared to 26.86 kW from the manufacturer's data. The comparison results can demonstrate the reasonable accuracy of the developed CFD model.

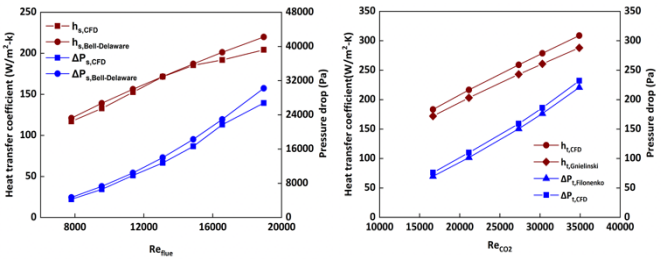

(a) (b)

Fig. 3. Comparasions of shell and tube side heat transfer coefficients and pressure drops

6. SIMULATION RESULTS

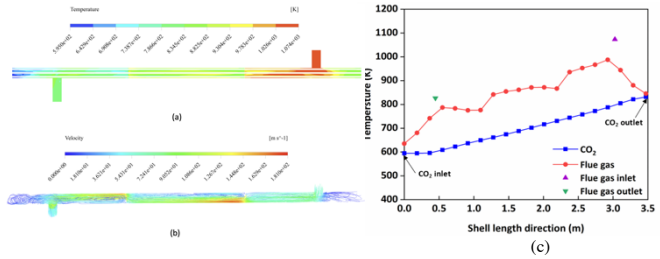

(c)

Fig. 4 Flue gas temperature contour (a) , velocity streamline (b), and CO_2 and flue gas temperature profiles along shell length direction (c)

From the CFD simulation results, across the mid-plane of the heat exchanger, the flue gas temperature contours and velocity streamlines are shown in Fig. 4(a) and 4(b) respectively. Meanwhile, the temperature profiles of flue gas and CO_2 fluid along the tube-length direction are demonstrated in Fig.4 (c). In addition, the positions and temperatures of flue gas inlet and outlet are indicated in Fig. 4(c). These results are based on the operating condition of flue gas mass flow rate at 0.12 kg/s and inlet temperature at 1073.15 K, CO_2 mass flow rate at 0.12 kg/s, CO_2 pressure at 12Mpa and inlet temperature at 595 K. It is seen that the CO_2 fluid temperature increases smoothly from its inlet to the outlet. However, the flue gas temperature decrease from its inlet to outlet is disrupted by those two baffles located at 1.1 m and 2.2 m along the shell tube direction. In addition, it is observed that there are two stagnated regions for the shell-side flue gas in which one is between CO_2 fluid inlet and flue gas outlet and another is between

the flue gas inlet and CO_2 fluid outlet. The flue gas temperatures in these two stagnated regions are relatively low such that the heat transfer between the flue gas and CO_2 fluid in these two regions are not significant. To enhance the heat transfer, it is thus suggested that the locations of flue gas inlet and outlet port pipes be installed as close as possible to each heat exchanger end.

The effects of flue gas inlet temperature and mass flow rate, CO_2 mass flow rate and pressure on the heat exchanger heat capacity are also simulated and shown in Fig.5. It should be noted that, in each simulation, except those two indicated variables, all other operating parameters are kept at their designed values as mentioned in section 2. As seen from the simulation results, higher flue gas temperature and flow rate, and higher CO_2 mass flow rate all contribute to higher heat capacity. This can be explained that the higher flue gas temperature can increase the CO_2 outlet temperature while the higher fluid flow rates can enhance the heat transfer of the heat exchanger. However, the effect of CO_2 pressure on the heat capacity is not that significant.

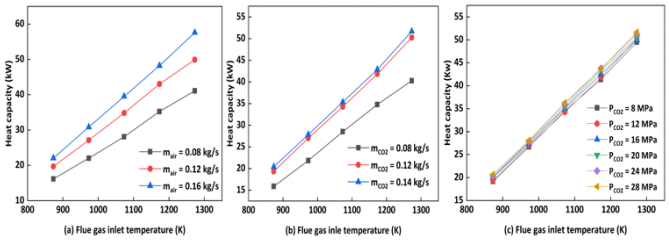

Fig.5. Heat capacity of CO_2 heat exchanger with various operating conditions

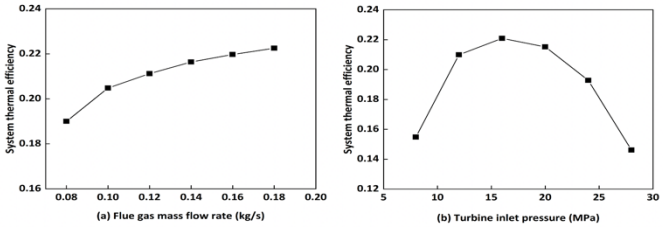

Fig. 6. Variation of system thermal efficiency with different flue gas mass flow rate and turbine inlet pressure at specificed heat source temperature of 1073.15 K.

The higher flue gas flow rate will also increase the system thermal efficiency due to the increased gas heater heat capacity, as shown in Fig. 6(a). However, similar to its effect on heat capacity, the increase extent of the thermal efficiency is reduced when the flue gas flow rate is further increased. Although the CO_2 pressure doesn't affect much to the gas heater heat capacity, there is an optimal CO_2 pressure to maximize the system thermal efficiency, as shown in Fig. 6(b). This is due to the opposite effect of CO_2 pressure on the turbine power generation and compressor power consumption when the CO_2 pressure at the turbine outlet is fixed. The simulation results can instruct well to the controls of gas heater and its associated system.

7. CONCLUSIONS

Detailed CFD model for a shell-and-tube supercritical CO_2 gas heater utilized in a biomass-CO_2 power generation system has been developed and validated. The validated model is then applied to predict the performance of the heat exchanger and its associated system at different operating conditions. It is found that the heat exchanger heat capacity increases with higher flue gas temperature and flow rate and higher CO_2 mass flow rate. However, the effect of CO_2 pressure on the heat exchanger heat capacity is insignificant. It is also observed from the simulation results that the locations of flue gas inlet and outlet port pipes significantly affect the heat transfer of the heat exchanger which can be improved in the heat exchanger design. In addition, the installations of baffles can also affect the heat transfer of the heat exchanger. Furthermore, both flue gas mass flow rate and CO_2 pressure affect significantly the system thermal efficiency which can be considered in the system optimal control strategies.

ACKNOWLEDGEMENT

The authors would like to acknowledge the support received from Ashwell Biomass Ltd, Research Councils UK (RCUK) and Innovate UK for this research project.

REFERENCE

[1] Kim WK, Aicher T. Experimental investigation of heat transfer in shell-and-tube heat exchangers without baffles. Korean Journal of Chemical Engineering 1997; 14(2):93-100.

[2] Halle H, Chenoweth J. and Wambsganss M. Shellside Waterflow Pressure Drop Distribution Measurements in an Industrial-Sized Test Heat Exchanger. Journal of Heat Transfer 1988; 110(1):60-67.

[3] Sparrow E, Reifschneider L. Effect of interbaffle spacing on heat transfer and pressure drop in a shell-and-tube heat exchanger. International Journal of Heat and Mass Transfer 1986; 29(11):1617-1628.

[4] Bell KJ. Delaware method for shell side design. Heat exchangers: thermal-hydraulic fundamentals and design. Hemisphere 1981; 581-618.

[5] Kern DQ . Process heat transfer (Vol. 5). New York: McGraw-Hill 1950.

[6] Gaddis E, Gnielinski V. Pressure drop on the shell side of shell-and-tube heat exchangers with segmental baffles. Chemical Engineering and Processing: Process Intensification 1997; 36(2): 149-159.

[7] Gnielinski V. New equations for heat and mass transfer in turbulent pipe and channel flow. Int. Chem. Eng. 1976; 16(2):359-368.